DALTON
FULL PAPER

Stereochemistry in solution of spiro-2,2′-dioxybiphenyl-cyclotriphosphazenes: an NMR spectroscopic study combined with molecular dynamics simulations

Maria E. Amato,[a] Gabino A. Carriedo,[b] Francisco J. Garcia Alonso,[b] Jose L. García-Alvarez,[b] Giuseppe M. Lombardo[c] and Giuseppe C. Pappalardo*[c]

[a] *Dipartimento di Scienze Chimiche, Università di Catania, Viale A. Doria 6, 95125 Catania, Italy*
[b] *Departamento de Química Orgánica e Inorganica, Facultad de Química, Universidad de Oviedo, Oviedo 33071, Spain*
[c] *Dipartimento di Scienze Chimiche, Cattedra di Chimica Generale, Facoltà di Farmacia, Università di Catania, Viale A. Doria 6, 95125 Catania, Italy. E-mail: gcpappalardo@dipchi.unict.it*

Received 27th February 2002, Accepted 29th May 2002
First published as an Advance Article on the web 2nd July 2002

The stereochemistry in solution of spirocyclophosphazenes **1**–**3** containing 2,2′-dioxybiphenyl groups, tris(2,2′-dioxybiphenyl)cyclotriphosphazene $[N_3P_3(O_2C_{12}H_8)_3]$ (**1**) and the chloro derivatives $[N_3P_3Cl_2(O_2C_{12}H_8)_2]$ (**2**) and $[N_3P_3Cl_4(O_2C_{12}H_8)]$ (**3**), was studied using high field ^1H, ^{13}C and ^{31}P NMR spectroscopy (variable temperature experiments) combined with molecular dynamics (MD) simulations. The ambient temperature spectra, after full assignments, showed a unique set of signals (four and six for hydrogens and carbons, respectively) for the corresponding nuclei of all the biphenoxy systems. This isochrony was compatible with symmetry equivalence as well as with fast interconversions on the NMR time scale between the stereoisomers *RRR*, *SSS*, *RRS*, *SSR* (**1**), *RR*, *SS*, *RS*, *SR* (**2**) and *R*, *S* (**3**). Dynamic NMR studies evidenced that atropoisomers of **1**–**3** are populated at low temperature (≤ 183 K) bearing out fast racemization of the $NP(O_2C_{12}H_8)$ units in solution at ambient temperature. The MD trajectories, which were long enough (50 ns) to monitor time-averaged processes on the NMR scale, were selectively compatible with DNMR results, and provided insights into the motional properties of **1**–**3**. They significantly complemented the experimental information on the exchange process of **3**, due to the inherent limitation of the single use of the NMR technique when NMR active diastereotopic nuclei are absent in the investigated system.

Introduction

Spirocyclophosphazenes comprise a special class of cyclic phosphazenes that have several aspects of interest, such as their ability to act as host molecules[1–7] and to induce inclusion polymerization.[2] Well known examples are the spirophosphazenes containing 2,2′-dioxybiphenyl groups **1**, **2** and **3** (Scheme 1), respectively referred as the tris-spiro,[8,9] the bis-spiro[9–12] and the mono-spiro[9,10] derivatives. Because of the presence of reactive P–Cl bonds, the compounds **2** and **3** have been used as precursors for many other derivatives such as condensation polymers,[11,12] or cyclophosphazenes carrying transition metal complexes[13] and polyradicals[14] that are appropriate models to evaluate electronic transmission through the –N=P–N= bonds in the N_3P_3 rings.

The crystal structures of **1**,[8] **2**[12] and the fluorine analogue of **3**,[15] have been determined by X-ray diffraction, and that of **3** is in progress in our laboratory. They have also been studied by vibrational,[16,17] and by ^{15}N NMR spectroscopies.[18] However, their stereochemical behavior in solution has not yet been completely elucidated.

The 2,2′-dioxybiphenylphosphazene unit $NP(O_2C_{12}H_8)$ may adopt the two conformations *R* and *S* shown in Fig. 1, giving rise to various stereoisomers for **1** (*RRR*, *RRS*, *RSS*, *SSS* and C_3 equivalent structures *RSR*, *SRS*, *SRR*, *SSR*), **2** (*RR*, *RS*, *SS*)S) and **3** (*R*, *S*) (Fig. 2), that may be rapidly interconverting in solution. By contrast, for the 2,2-binaphthoxy analogues, the interconvertion has a much larger energy barrier, and therefore the optically active pure atropoisomers *RRR* or *SSS* of tris(2,2′-dioxy-binaphthyl)cyclotriphosphazene {(+)-$[N_3P_3(O_2C_{20}H_{12})_3]$ could be isolated[19] and characterized in the amorphous solid state by EDXD and molecular dynamics (MD).[20]

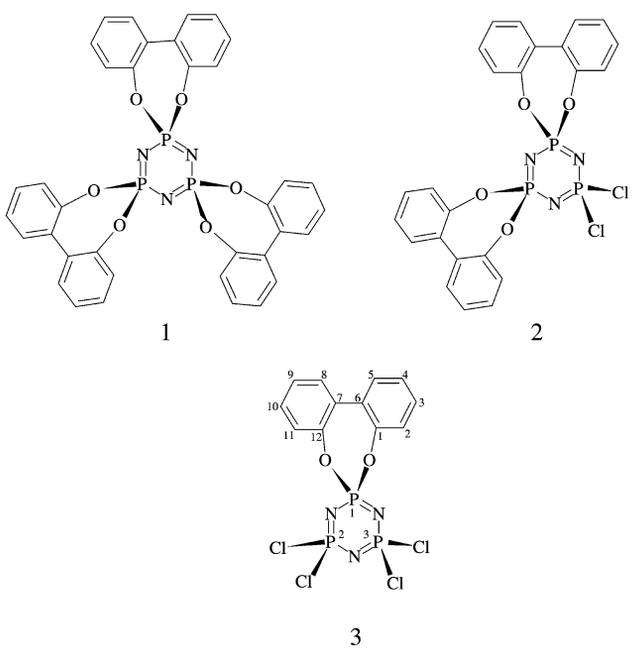

Scheme 1

DOI: 10.1039/b202083c

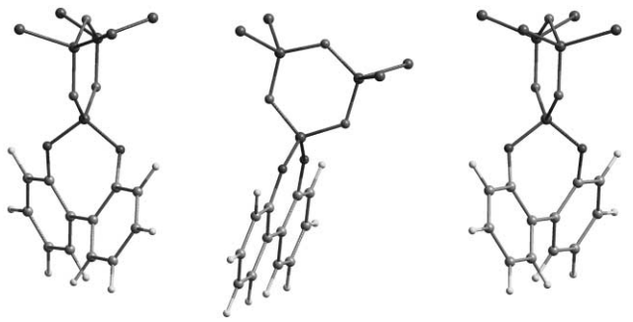

Fig. 1 View of **3** showing the enantiomeric conformations *R* (a) and *S* (c) achieved by clockwise and anti-clockwise twistings, $\phi = 41°$ and $\phi = -41°$, respectively of the phenyl rings of the $NP(O_2C_{12}H_8)$ unit on passing through coplanarity of the seven-membered aryldioxyphosphole ring C1–C6–C7–C12–O–P1–O at the transition state (b).

In spite of the expected different stereoisomers for **1** in solution, only one was found in the crystal, which was attributed to the packing forces.[8] Analogously, only the *meso* diastereomer (*R*,*S*) was observed in the crystal structure of **2**, but in this case it was attributed to the specific formation of this diastereomer in the reaction beetween $[N_3P_3Cl_6]$ and two equivalents of 2,2′-dioxybiphenyl.[12]

In principle, as found in several substituted derivatives of **2** with $-OC_6H_4-R$ groups (R = NO_2, NH_2, $NHCOCH_3$)[11] the diastereoisomers of **1**, **2** and **3** could be distinguished by NMR spectroscopy. However, the occurrence of interconversion processes between stereoisomers of these spirophosphazenes is an issue, and their corresponding dynamics and energetics are also unanswered. In this work high-field ^1H, ^{13}C and ^{31}P NMR variable temperature experiments, including preliminary complete spectral assignments, were performed to address the above questions.

The results were complemented by molecular dynamics (MD) simulations.[21] The MD technique calculates the time dependent movement of each atom in a molecule. The changes in velocities and coordinates with time are recorded in trajectories. Application of MD for simulating the spiro-2,2′-dioxybiphenyl-cyclotriphosphazenes **1**–**3** would provide the ability to monitor the internal molecular fluctuations. Mainly due to limits in computing power and data storage, the length of MD simulations is limited to hundreds of picoseconds or nanoseconds at most. For this reason MD may be in general less effective for crossing large energy barriers as well as for reproducing processes that are fast with respect to the NMR time-scale. To accomplish this one must ensure that the molecular simulations are carried out on a long enough time-scale to sample a significant volume of phase space. In this work the MD runs were long enough (50 ns) to generate microscopic-level information (exchange between molecular states) for direct correlation with experimental NMR results (variable temperature spectra). Until now MD has provided the capability to help refinement of molecular structures using NMR data such as NOE intensities, relaxation times and coupling constants in the liquid phase.

Experimental

Samples

The compounds **1** to **3** were prepared as described elsewhere.[9]

NMR spectroscopy

The room temperature ^1H (499.88 MHz) and HSQC NMR experiments were carried out at 300 K on a Varian UNITY Inova 500 spectrometer equipped with a pulse field gradient module (*Z* axis) and a tunable 5 mm Varian inverse detection probe (ID-PFG). Acquisition parameters for ^1H spectra were: pulse width 7.1 μs, acquisition time 2.7 s, relaxation delay 2 s, spectral width 6 kHz, 32 K data points. The phase-sensitive HSQC sequence was used as provided in the Varian software library. The spectra were obtained with the following parameters: ^1H spectral window of 5 kHz, 1k data point in f_2, ^{13}C (f_1) spectral window of 12 kHz, 256 time increments in f_1 zero filled to 512. The relaxation delay was 2 s, 32 spectra were collected per time increment and ^{13}C GARP decoupling was applied during acquisition. Gaussian weighting was applied to the raw data and to the t_1 interferograms prior to Fourier transformation.

The variable temperature ^{13}C (125.7 MHz) and ^{31}P (202.35 MHz) were acquired by using a tunable 5 mm BB Varian probe. Acquisition parameters for $^{13}C\{^1H\}$ spectra were: pulse width 5.85 μs (45° pulse), acquisition time 1.1 s, relaxation delay 2 s, spectral width 30 kHz, 64k data points and 0.45 Hz spectral resolution. Acquisition parameters for $^{31}P\{^1H\}$ spectra were: pulse width 5.4 μs (30° pulse), acquisition time 0.8 s, relaxation

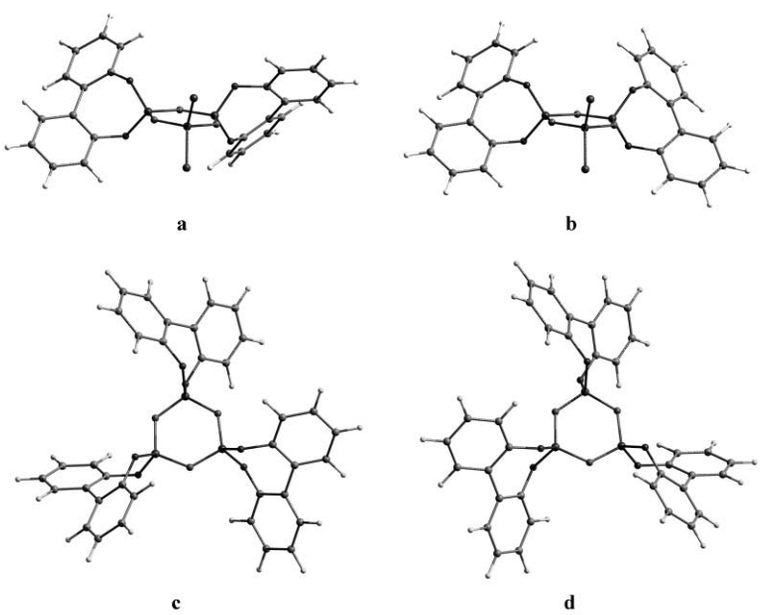

Fig. 2 Views of the *SS* (a) and *SR* (b), and of the *RRR* (c) and *RSS* (d) atropoisomers of **2** and **1**, respectively. The views do not include the remaining forms *RR* and *RS* of **2**, and *SSS*; *RRS*, *RSR*, *SRR*, *SRS*, *SSR* of **1**, that are attainable by simple reflection and/or rotation.

delay 20 s, spectral width 16 kHz, 32k data points and 1.2 Hz spectral resolution.

The variable-temperature ^{1}H NMR data were acquired using tunable 5 mm Varian inverse detection probe (pulse width 7.8 μs). Samples were dissolved in $CDCl_3$ or CD_2Cl_2; the chemical shifts (ppm) were referenced to external TMS (^{1}H and ^{13}C) or to external 85% H_3PO_4 (^{31}P) and were positive in the low field direction from the standards.

Theoretical methods

MD simulations. The Cerius^2 package developed by BIOSYM/MSI was used to perform all the MD calculations through the OFF (Open Force Field) routine that includes the empirical functions of the CHARMm force field.[22] The force field (FF) techniques for phosphazenes require a suitable set of parameters for all the internal coordinates of the uncommon structural units in these materials. The CHARMm FF parameter set was derived by us previously for tris(2,2′-dioxybinaphthyl)cyclotriphosphazene[20] and poly-bis(chloro)-phosphazene,[23] using the technique of energy derivatives obtained from *ab initio* quantum mechanics (at the Hartree–Fock level with 6-31G* basis set) as outlined by Dinur and Hagler.[24] The atomic charges (ranges: P, 1.16/0.52; N, −0.10/−0.49; O, −0.45/−0.51; C, −0.16/0.32; H, 0.06/0.14; Cl, −0.19/−0.44) were obtained with the charge equilibration method implemented in the Cerius^2 package.[25] The NB interactions cut-off was implemented according to the SPLINE method as a function of the interatomic distances (r) as follows: for $r <$ SPLINE-ON = 10 Å, fully considered; for $r >$ SPLINE-OFF = 15 Å, fully ignored; for SPLINE-ON $< r <$ SPLINE-OFF, reduced in magnitude. The dielectric constant was set to $\varepsilon = 1$. Preliminary checks showed that the total relative energies and twisting barriers were unaffected with respect to those calculated using distance-dependent ε.

All the simulations were carried out in the gas phase using Nosé's NVT (constant temperature) algorithm.[26] Starting from energy-minimized structures obtained through the conjugate gradient method and satisfying a gradient of ≤0.001 kJ mol^{-1} Å^{-1}, MD simulations were run at temperatures of 180, 210, 300 and 350 K, with a thermal bath coupling constant set at 0.1 ps. For each temperature, after a heating phase of 100 ps, transients of 50 ns (number of MD steps = 5×10^7) with a sampling interval of 2 ps were usually collected. The integration time step was set at 0.001 ps.

Results and discussion

A process of exchange between the stereoisomeric forms in the 2,2′-dioxybiphenyl cyclophosphazenes **1**–**3**, if it occurs in solution, involves a 2,2′-dioxybiphenyl group jumping between the right handed ($+\phi$) and left handed ($-\phi$) helical conformations. The exchange process between these enantiomeric conformations of the $NP(O_2C_{12}H_8)$ unit occurs on passing through coplanarity of the phenyl rings and simultaneous motion of the O–P–O bridge (Fig. 1). The free energy of activation for the *R*–*S* interconversion therefore depends on the degree to which the bridge restricts the freedom of torsion about the C6–C7 inter-ring axis of the 2,2′-dioxybiphenyl group. Accordingly, the racemic *RR*/*SS* and *meso SR*/*SR* forms, *e.g.* in the case of **2**, correspond to the conformations represented by right-handed (+) and left-handed (−) twisting about the biphenoxyl C6(1)–C7(1) and C6(2)–C7(2) bonds (Fig. 2). It follows that the atropoisomerization process of the stereogenic biphenoxy units can be monitored *via* DNMR because diastereoisomeric forms of **2** (and **1**) are expected to show distinct signals for the active nuclei.

The sample **3**, although lacking the necessary presence of NMR active diastereotopic nuclei, was included in the studied series, because information otherwise inaccessibile on such a spirocyclophosphazene bearing a single $NP(O_2C_{12}H_8)$ fragment was foreseen by analogy with **1** and **2** and by the presently used combined experimental and theoretical approach.

Every ^{1}H spectrum of **1**–**3** showed, at ambient as well as at higher temperatures, a unique set of four signals (Fig. 3) which were assigned, based on chemical shift considerations and multiplicities, to the nuclei of each aromatic ring of the biphenoxy systems. The spectral assignments (Table 1) showed consistency with reported data for 2,2′-substituted biphenyls.[27] The splitting patterns of **3** evidenced long range couplings J_{H-P} of 1.5 Hz (max) in all proton signals (Table 1).

The use of HSQC experiments made straightforward the assignments of the 125 MHz ^{13}C NMR spectra. Quaternary carbon signals C1 and C6 were attributed on the basis of chemical shift considerations. The spectra of **1**–**3**, showing each a pattern of six signals due to the aromatic carbons, denoted, analogously to the hydrogen's pattern, isochrony between corresponding aromatic nuclei of all the biphenoxy groups in each sample. The carbon signals of **1** and **2** resonated as singlets with the exception of C1 and C2 coupled to the phosphorus nuclei. The signals of C1 and C2 of **3** appeared as doublets separated by 9.5 and 4.9 Hz, respectively, in good agreement with previous work[9] using a spectrometer operating at lower field. Moreover, the remaining C3, C4 and C5 signals of **3** were also doublets arising from smaller $^{n}J_{C-P}$ coupling constants ranging from 1.6 to 2.37 Hz. The ^{31}P spectra of **1**–**3** well reproduced the previously reported sets of signals.[9,18]

The low temperature ^{1}H spectra of **1**–**3** in $CDCl_3$ showed a general progressive small downfield shift of the H2, H3, and H4 nuclei. The H2 and H3 line widths of **1** increased significantly below about 248 K, and merged the H4 signal into a unique broad line at 218 K (Fig. 3a). The H2, H3, and H4 signals of **2** broadened below 238 K (Fig. 3b). At 218 K, the spectral pattern of **3** slightly broadened (Fig. 3c), and the $^4J_{H-H}$ and J_{H-P} couplings became undetectable. The chemical shift and line width of the H5 signal of **1**–**3** in $CDCl_3$ remained substantially unaffected by the temperature changes (Fig. 3).

On cooling below 300 K, the 125.7 MHz ^{13}C NMR spectrum of **2** in $CDCl_3$ solution showed progressive broadening of the C2, C3 and C6 signals. At 228 K, the line-width of C2 rose up to about 40 Hz, and at 213 K the signal separated into two broad signals as well as those of C3 and C6 (Fig. 4). An absence of temperature effects was observed on the ^{13}C spectrum of **3** in the range 213–300 K. The ^{13}C spectrum of **1** was recorded only at 300 K, due to the relatively low solubility of the sample.

The ^{31}P spectra of **1**–**3** showed a small line width increase on decreasing temperature. The most significant effect (from 1.7 to 12.4 Hz, on cooling from 300 to 218 K, respectively) was detected for the P1/P2 signal of **2**.

All the spectral changes observed were reversible and thus consistent with a process of atropoisomerization of the biphenoxy moieties in **1** and **2**. The same process may be inferred for **3** by considering that near magnetic equivalence between corresponding nuclei is likely to occur in both the *R* and *S* stereoisomers.

In order to explore a wider range of temperatures, the ^{13}C spectra of **2** were also recorded in CD_2Cl_2 solution. At room temperature, the same pattern and multiplicity of signals was observed as in $CDCl_3$ (Fig. 5). On cooling between 300 and 205 K, all signals, except C1, progressively broadened. The most significant line broadening was detected for the C2 signal (*ca.* 20 Hz) which sharpened again at lower temperature (below 203 K). At 193 K, new broad resonances appeared for C2, C3, C4 and C6. The C3 resonance was separated into two signals, one of which was superimposed onto the C5 signal whereas the upfield one was further separated into two lines. Below about 183 K, line broadening was detected also for C1 and C5 (Fig. 5).

The ^{1}H NMR spectrum of **2** in CD_2Cl_2 displayed four well resolved aromatic signals at room temperature. On lowering

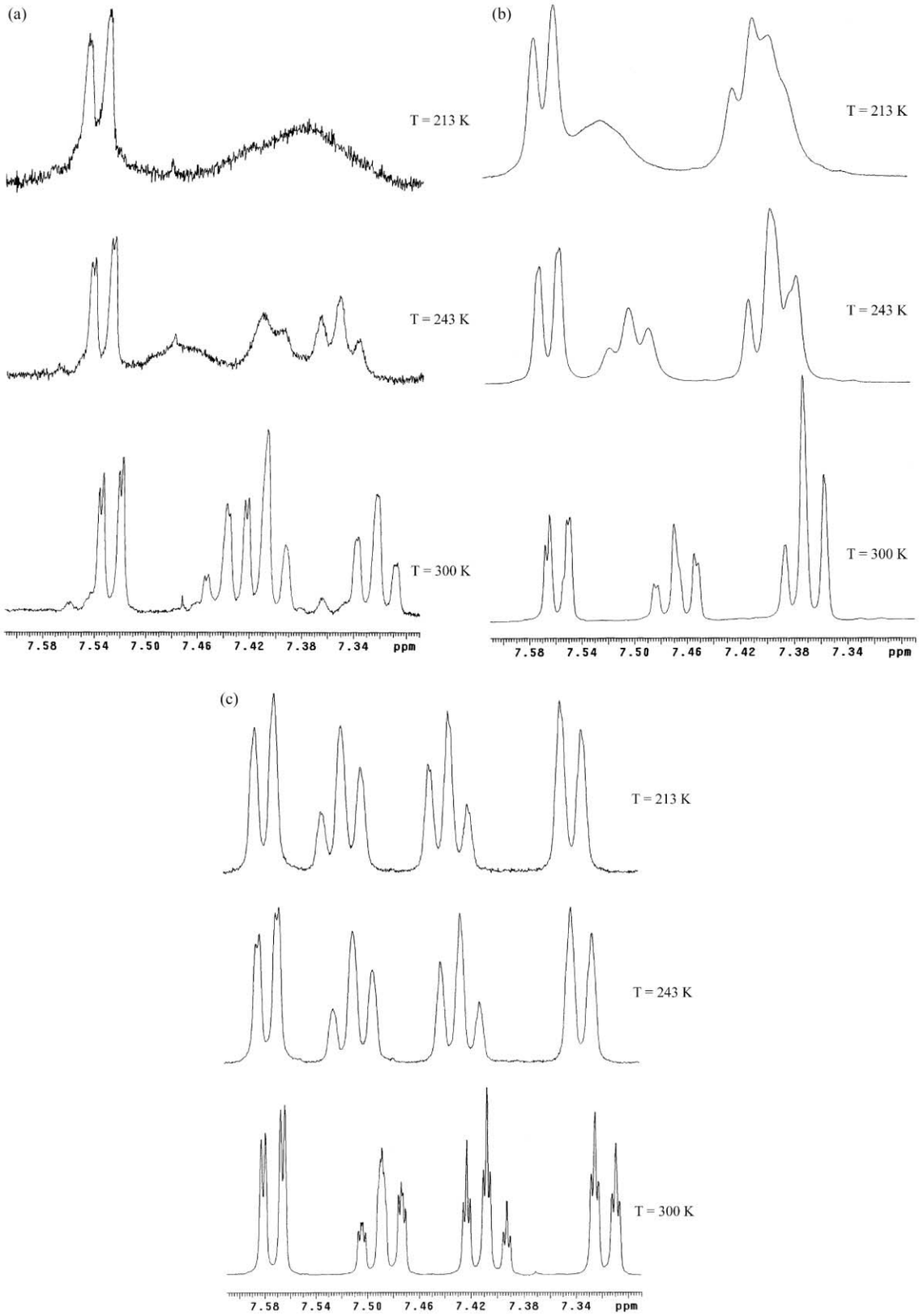

Fig. 3 Temperature-dependent ^{1}H NMR spectra (500 MHz) of **1** (a), **2** (b) and **3** (c) in $CDCl_3$ solution.

the temperature they broadened and at 193 K, H2 signal decoalesced into two lines, the upfield one being clearly distinguishable. At 183 K, all signals were broad but clearly duplicated (Fig. 6a).

The ^{1}H spectrum of **1** in CD_2Cl_2, well resolved at room temperature, at 213 K showed a very broad line which merged H2, H3 and H4 signals, whereas at 183 K, the broadened lines reattained resolution in peaks providing evidence that separate states are frozen at this temperature (Fig. 6b).

To attain more information about the microscopic properties determining the found temperature effect on the NMR spectra, the sampling of the conformational space associated with the molecules **1**–**3** was performed through use of MD simulations. The trajectories were spanned for sufficiently large evolution time to reveal processes that are averaged on the NMR timescale. The analyses of the trajectories made in terms of the fluctuations about the torsion angle ϕ showed the occurrence at ambient temperature of interconversions between enantiomeric

Table 1 ^{1}H and ^{13}C NMR data for cyclospirophosphazenes **1**–**3** at 300 K: chemical shifts (δ, in ppm from TMS); multiplicities (in parentheses); coupling constants (J, in Hz)

	1			**2**				**3**	
Solvent	$CDCl_3$		CD_2Cl_2	$CDCl_3$		CD_2Cl_2		$CDCl_3$	
Atom	^{1}H	^{13}C	^{1}H	^{1}H	^{13}C	^{1}H	^{13}C	^{1}H	^{13}C
1 (12)	—	148.23 (m)	—	—	147.75 (t)		147.88	—	147.3 (d, 9.5)
2 (11)	7.42 (d)	122.01 (m)	7.41 (d)	7.36 (d)	121.82 (t)	7.37 (dd)	121.85	7.316 (td) [a]	121.72 (d, 4.5)
3 (10)	7.44 (dt)	129.66 (s)	7.49 (dt)	7.47 (dt)	129.74 (s)	7.52	130.06	7.49 (tt) [b]	129.87 (d 1.4)
4 (9)	7.33 (dt)	126.124 (s)	7.4 (t)	7.37 (t)	126.49 (s)	7.43	126.85	7.41 (tt) [c]	126.87 (d, 2.26)
5 (8)	7.53 (dd)	129.75 (s)	7.61 (dd)	7.56 (dd)	129.98 (s)	7.62	130.26	7.57 (dd) [d]	130.19 (d, 1.38)
6 (7)		128.92 (s)		—	128.56 (s)		128.70		128.3 (d, 1.9)

[a] $J_{ortho} = 7.99$, $J_{meta} = 1.4$, $J_{para} < 1$, $J_{PH} < 1$. [b] $J_{ortho} = 7.6$, $J_{ortho} = 7.99$, $J_{meta} = 1.4$, $J_{PH} < 1$. [c] $J_{ortho} = 7.6$, $J_{ortho} = 7.49$, $J_{meta} = 1.4$, $J_{PH} = 1.5$. [d] $J_{ortho} = 7.49$, $J_{meta} = 1.4$, $J_{para} < 1$, $J_{PH} < 1$.

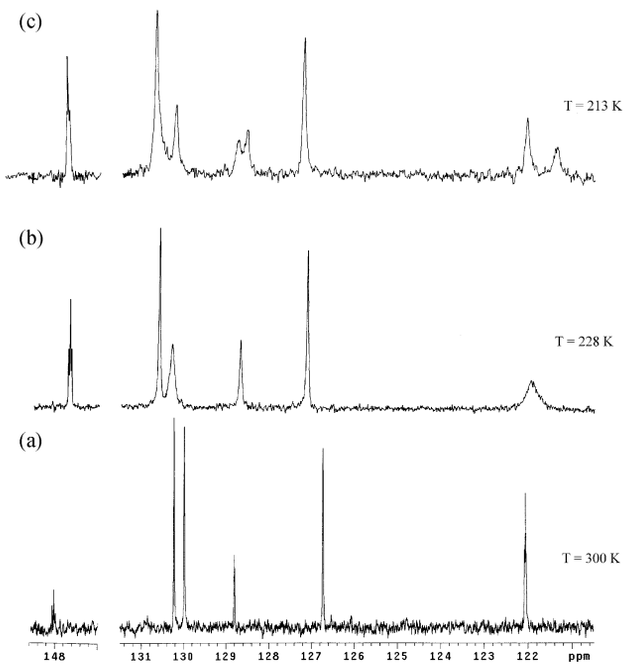

Fig. 4 Temperature-dependent ^{13}C NMR spectra (125.7 MHz) of **2** in $CDCl_3$ solution. The C2, C3 and C6 signals (singlets at room temperature, trace a) are broadened at 228 K (trace b) and each split into two lines at lower temperature. At 213 K some exchange broadening still occurs due to the C6/C7 rotation (trace c). In the temperature range examined, the remaining carbons give rise to sharp signals due to incidental degeneracy.

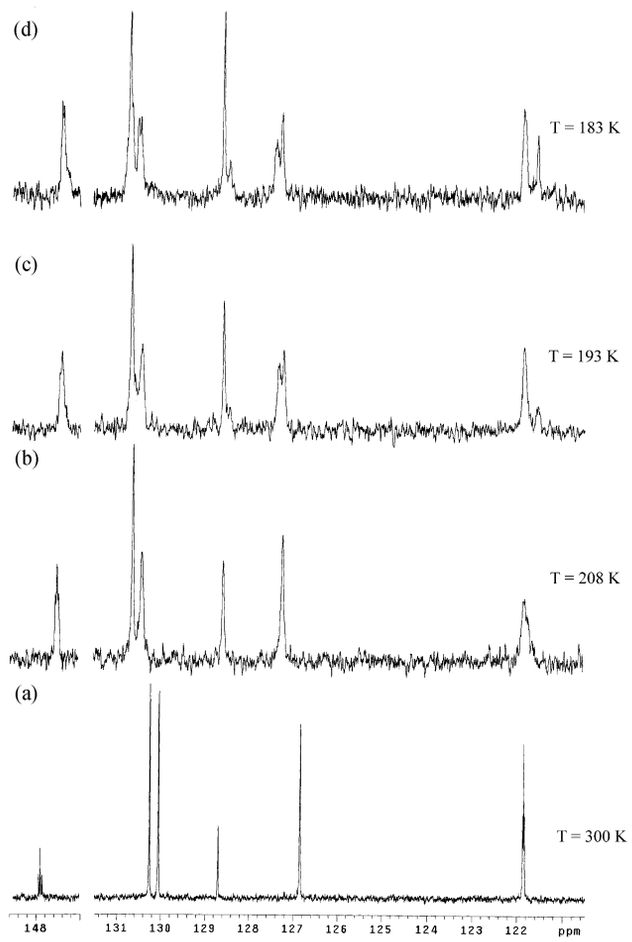

Fig. 5 Temperature-dependent ^{13}C NMR spectra (125.7 MHz) of **2** in CD_2Cl_2 solution. By amplifying the low-temperature traces (b–d) new resonances attributable to the presence of atropoisomeric conformations were evidenced. The relative signal intensities obtained at 180 K were determined both by conformer population and very closely spaced resonances of some of the corresponding carbons in the biphenoxy moieties in the diastereomers.

conformations of each 2,2′-dioxybiphenyl moiety of **1**–**3** (Fig. 7–9) corresponding to the equilibrium values of $\phi = 41°$ and $\phi = -41°$.

The MD simulated interconversion processes of each $NP(O_2C_{12}H_8)$ unit from *R* to *S* and *vice versa* become less frequent at lower temperatures, and the jumps completely disappeared at 183 K during the same evolution time.

Inspection of the trajectories (Fig. 7–9) shows, as first, that at room temperature all the possible diastereoisomeric forms of **1**–**3** are populated, and second, that the interconversion frequency rate of atropoisomerization decreases on passing from **1** to **2** and, in turn, from **2** to **3**, thus decreasing the number of 2,2′-dioxybiphenyl moieties. In addition, lifetimes of the atropoisomers *RRR* or *SSS* of **1** are longer than those of the *RRS* or *SSR* ones. This feature is retained in the case of the *RR* or *SS* enantiomers of **2**, whose lifetimes are longer than those of the *RS* or *SR* ones. This could be due to the relative energy difference between the energy minimized structures that favour (by about 1 kcal mol^{-1}) the *RRR*/*SSS* and *RR*/*SS* atropoisomers with respect to the *RRS*/*SSR* and *RS*/*SR* ones, respectively (Table 2). The calculated *R* to *S* twisting barriers for a single 2,2′-dioxybiphenyl moiety in **3**, **2** and **1** were 4.82, 5.6 and 5.3 kcal mol^{-1}, respectively.

The important feature of the MD trajectories of **2** was the lack of simultaneous jumps of both biphenoxy moieties to determine the exchange from a *meso*-(*RS*)S) to the other *meso*-(*SR*) atropoisomer (Fig. 8). This is in agreement with experimental evidence because a simultaneous exchange will not produce the found chemical shift changes after cooling (decoalescence).

On the basis of the above results the alternate possibility of symmetry equivalence compatible with ambient temperature

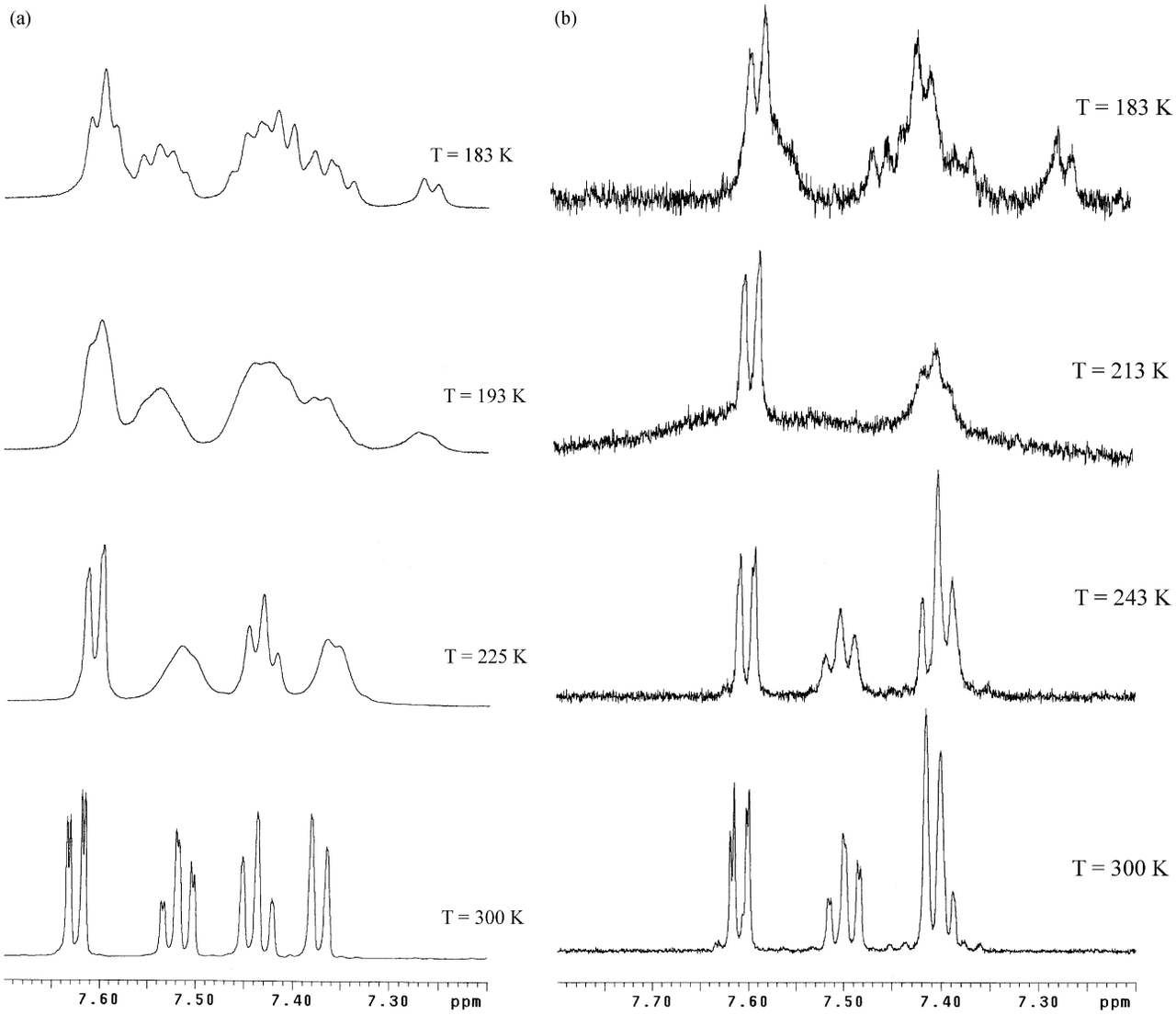

Fig. 6 Temperature-dependent ^{1}H NMR spectra (500 MHz) of **2** (a) and **1** (b) in CD_2Cl_2 solution.

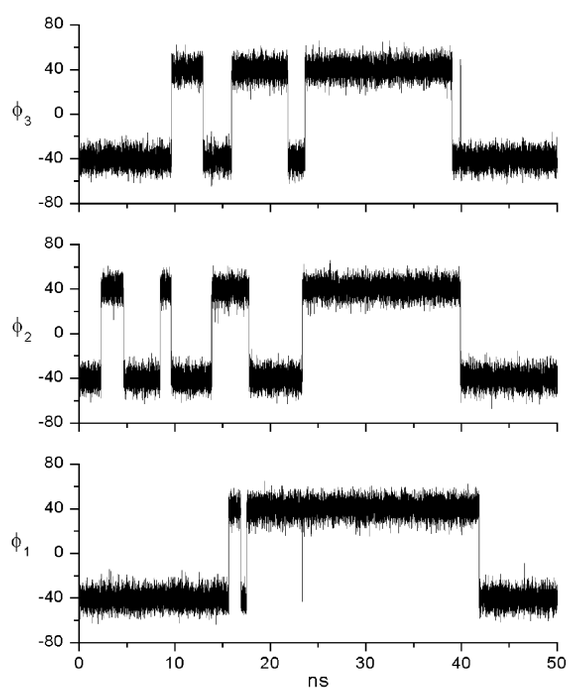

Fig. 7 Time evolution traces for the ϕ_1, ϕ_2 and ϕ_3 twisting angles of the $NP(O_2C_{12}H_8)$ units from MD simulation of **1**.

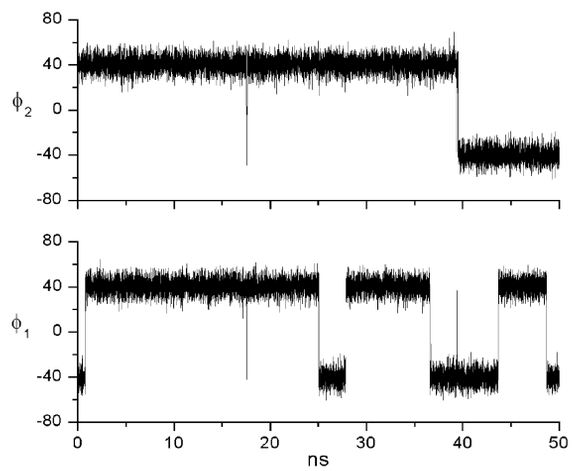

Fig. 8 Time evolution traces for the ϕ_1 and ϕ_2 twisting angles of the $NP(O_2C_{12}H_8)$ units from MD simulation of **2**.

NMR experiments can be safely ruled out. The MD results also do not contrast with the expected lack of chemical shift differences on cooling the solution of **3**, for which, by analogy with **1** and **2**, a fast exchange process can be deduced. Also the observed temperature dependent line broadening of the ^{31}P spectra can be rationalised in terms of chemical shift differences between the stereoisomers smaller than the line widths. The evolution traces given in Fig. 9 show that the conformational

Table 2 Optimized energies (kcal mol^{-1}) of stereoisomers of **1**–**3** as calculated by the force field method

	1		**2**		**3**
Energy	*RRR*	*RRS*	*RR*	*RS*	*R*
Total	172.724	173.441	119.890	120.443	−31.286
Bonds	5.241	5.329	4.664	4.753	3.530
Angles	14.708	14.900	15.540	15.743	16.585
Dihedral	96.625	96.129	58.328	57.901	19.404
Improper	0.216	0.220	0.136	0.139	0.054
Urey–Bradley	7.280	7.500	7.573	7.777	8.922
Van der Waals	28.553	28.136	18.159	18.047	7.707
Electrostatic	20.102	21.227	15.490	16.081	−87.489

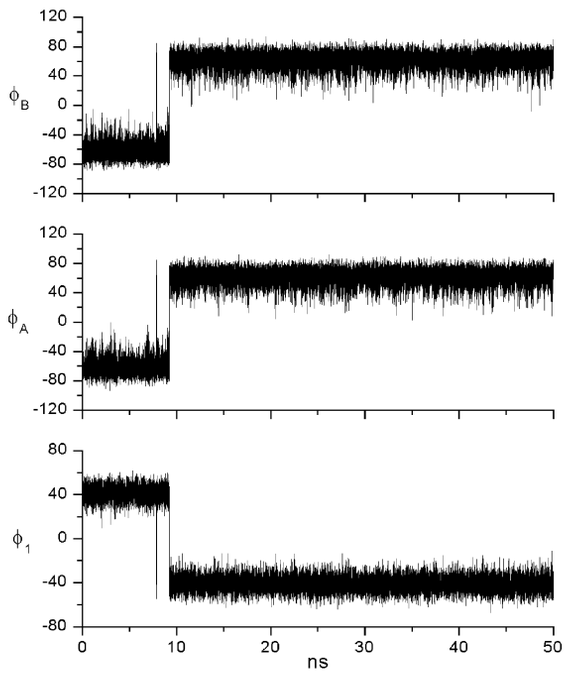

Fig. 9 Time evolution trace for the ϕ_1 twisting angle of the $NP(O_2C_{12}H_8)$ unit from MD simulation of **3**. The upper traces refer to the torsional angles P1–O–C1–C6 (ϕ_A) and P1–O–C12–C7 (ϕ_B) of the seven-membered aryldioxyphosphole ring C1–C6–C7–C12–O–P1–O simultaneously jumping from *ca.* −60° to +60°.

interconversion of the seven-membered aryldioxyphosphole ring C1–C6–C7–C12–O–P1–O occurs simultaneously to the jump of ϕ_1 from 40° to −40°, and thus on passing from the *R* to the *S* form.

The MD simulations thus agree fairly well with the experimental results in terms of fast exchange processes active at ambient probe tempertatures, and frozen at 183 K.

Conclusions

Variable temperature ^{1}H, ^{13}C and ^{31}P NMR experiments combined with MD simulations provide evidence that all the possible stereoisomers [*RRR*, *SSS*, *RRS*, *RSR*, *SRR*, *SRS*, *SSR*, *RSS* (**1**), *RR*, *SS*, *RS*, *SR* (**2**) and *R*, *S* (**3**)] of the spirocyclotriphosphazenes **1**–**3** are populated in solution. The dynamic exchange between the atropoisomers is fast on the NMR time scale at ambient temperature. The possible hypothesis of symmetry isochrony between pairs of chemically equivalent nuclei on the phenyl groups of each $NP(O_2C_{12}H_8)$ unit in the **1**–**3** spirocyclophosphazenes was ruled out. The MD results were fairly consistent with the NMR spectral changes observed on cooling the solutions. This enabled us to further use the MD technique to provide, in complementary fashion, otherwise inaccessible microscopic level information on the exchange processes of **3**.

It follows that the single diasteroisomers found[8,12] for the **1** (*SSR*/*SRR*) and **2** (*meso*) molecules in the crystalline state mainly result from crystal packing forces.

Acknowledgements

Work supported by MURST-PRIN 99–01 (Italy), and by DGICYT-Project 98–PB97–1276 (Spain).

References

1 H. R. Allcock, A. P. Primrose, N. J. Sunderland, A. L. Rheingold, I. A. Guzei and M. Parvez, *Chem. Mater.*, 1999, **11**, 1243.
2 H. R. Allcock, E. N. Silverberg, G. K. Dudley and S. R. Pucher, *Macromolecules*, 1994, **27**, 7550.
3 H. R. Allcock, R. W. Allen, E. C. Bissell, L. A. Smeltz and M. Teeter, *J. Am. Chem. Soc.*, 1976, **98**, 5120.
4 P. Sozzani, A. Comotti, R. Simonutti, T. Meersmann, J. W. Logan and A. Pines, *Angew. Chem., Int. Ed.*, 2000, **39**, 2695.
5 H. R. Allcock, N. J. Sunderland, A. P. Primrose, A. L. Rheingold, I. A. Guzei and M. Parvez, *Chem. Mater.*, 1999, **11**, 2478.
6 A. Comotti, M. C. Gallazzi, R. Simonutti and P. Sozzani, *Chem. Mater.*, 1998, **10**, 3589.
7 H. R. Allcock, A. P. Primrose, E. N. Silverberg, K. B. Visscher, A. L. Rheingold, I. A. Guzei and M. Parvez, *Chem. Mater.*, 2000, **12**, 2530.
8 H. R. Allcock, M. T. Stein and J. A. Stanko, *J. Am. Chem. Soc.*, 1971, **93**, 3173.
9 G. A. Carriedo, L. Fernández-Catuxo, F. J. García Alonso, P. Gómez Elipe and P. A. González, *Macromolecules*, 1996, **29**, 5320.
10 R. A. Pelc, K. Brandt and Z. Jedlinski, *Phosphorus, Sulfur Silicon Relat. Elem.*, 1990, **47**, 375.
11 D. Kumar and A. D. Gupta, *Macromolecules*, 1995, **28**, 6323.
12 I. Dez, J. Levalois-Mitjaville, H. Grützmacher, V. Gramlich and R. de Jaeger, *Eur. J. Inorg. Chem.*, 1999, 1673.
13 G. A. Carriedo, F. J. García Alonso, J. L. García, R. J. Carbajo and F. López Ortiz, *Eur. J. Inorg. Chem.*, 1999, 1015.
14 G. A. Carriedo, F. J. García Alonso, P. Gómez Elipe, E. Brillas and L. Juliá, *Org. Lett.*, 2001, **3**, 1625.
15 A. Vij, S. J. Geib, R. L. Kirchmeier and J. M. Shreeve, *Inorg. Chem.*, 1996, **35**, 2915.
16 G. A. Carriedo, F. J. García Alonso, P. A. González and J. R. Menéndez, *J. Raman Spectrosc.*, 1998, **29**, 327.
17 J. R. Menéndez, G. A. Carriedo, F. J. García Alonso, E. Clavijo, M. Nazri and R. Aroca, *J. Raman Spectrosc.*, 1999, **30**, 1121.
18 E. Peláez Arango, F. J. García Alonso, G. A. Carriedo and F. López Ortiz, *J. Magn. Reson., Ser. A*, 1996, **121**, 154.
19 G. A. Carriedo, F. J. García Alonso, P. A. González and J. L. García Alvarez, *Macromolecules*, 1998, **31**, 3189.
20 M. E. Amato, R. Caminiti, G. A. Carriedo, F. J. García Alonso, J. L. García Alvarez, G. M. Lombardo and G. C. Pappalardo, *Chem. Eur. J.*, 2001, **7**, 1486.
21 *Computer Simulations of Biomolecular Systems. Theoretical and Experimental Applications*, W. F. van Gunsteren, P. K. Weiner and A. J. Wilkinson, eds, Kluwer Academic Publishers, The Netherlands, 1997, vol. 3 and refs. therein.
22 B. R. Brooks, R. E. Bruccoleri, B. D. Olafson, D. J. States, S. Swaminathan and M. Karplus, *J. Comput. Chem.*, 1983, **4**, 187.
23 M. E. Amato, A. Grassi, K. B. Lipkowitz, G. M. Lombardo, G. C. Pappalardo and C. Sadun, *J. Inorg. Organomet. Polym.*, 1996, **6**, 237.
24 U. Dinur and A. T. Hagler, in *Reviews in Computational Chemistry*, K. B. Lipkowitz and D. B. Boyd, eds., VCH Publishers, New York, 1991, vol. 2, pp. 99–164.
25 A. K. Rappe and W. A. Goddard III, *J. Phys. Chem.*, 1991, **95**, 3358.
26 S. Nosé, *J. Chem. Phys.*, 1984, **91**, 511.
27 NMR Spectral Database, NIMCR (http://www.aist.go.jp/RIODB/SDBS/).